Original

Maier, P.; Richter, A.; Tober, G.; Hort, N.:

Effect of Grain Size and Structure, Solid Solution Elements, Precipitates and Twinning on Nanohardness of Mg-RE alloys

Materials Science Forum, Light Metals Technology Conference, LMT 2013 (2013)
Trans Tech Publications

DOI: 10.4028/www.scientific.net/MSF.765.491

Materials Science Forum *Online: 2013-07-31*
ISSN: 1662-9752, Vol. 765, pp 491-495
doi:10.4028/www.scientific.net/MSF.765.491

Effect of Grain Size and Structure, Solid Solution Elements, Precipitates and Twinning on Nanohardness of Mg-RE alloys

Petra Maier[1,a], Asta Richter[2,b], Gerhard Tober[1,c] and Norbert Hort[3,d]

[1]University of Applied Sciences Stralsund, Zur Schwedenschanze 15, 18435 Stralsund, Germany

[2]University of Applied Sciences Wildau, Bahnhofstraße, 15745 Wildau, Germany

[3]Helmholtz-Zentrum Geesthacht, Max-Planck-Strasse 1, D-21502, Geesthacht, Germany

[a]petra.maier@fh-stralsund.de, [b]asta.richter@th-wildau.de, [c]gerhard.tober@fh-stralsund.de, [d]norbert.hort@hzg.de

Keywords: Mg-RE alloys, Dendrites, Grain size, Twinning, Precipitates

Abstract. In this study Mg10GdxNd alloys are investigated by nanoindentation hardness measurements in several material conditions. Mg10GdxNd alloys with an average coarse grain size of 500 μm were cast by permanent mold direct chill casting. Hardness values vary due to the inhomogeneous microstructure formed during the solidification process consisting of dendrite arms with preferred orientation direction. The effect of dissolving particles during solution heat treatment (T4) and isothermal ageing (T6) was observed to a different extent depending on Nd content. Isothermal ageing promotes a duplex microstructure of coarse β_1 phase precipitates and regions containing much finer precipitates. Post processing by direct extrusion changes the microstructure dramatically to an average grain size of 15 μm. The microstructure after hot extrusion shows segregation of precipitates in the extrusion direction. Near this alignment of second phases hardness and plastic deformation differ from precipitates enriched in RE elements due to depleted regions of solid solution around them. This phenomenon is known from alloying element segregation to grain boundaries. Depending on the amount and location of second phases in the as-cast microstructure and degree of cold work, recrystallization leads to an inhomogeneous microstructure, consisting of fine grains (15 μm) and very fine grains, where second phases act as nuclei during the recrystallization process. Furthermore, mechanical testing (fatigue) causes an increase in dislocation density by work hardening and extensive twinning near the fractured surface. Here the hardening effect interferes with grain size strengthening.

Introduction

The good strength to weight ratio of Mg-RE alloys has led to an increasing research on these then as light weight construction materials [1]. They have also shown excellent creep resistance due to their good high temperature strength [2]. Furthermore Mg alloyed with RE elements is of interest for medical applications because of their adequate corrosion rate, such as biodegradable implants [3]. Creep and corrosion mechanisms are particularly influenced by local property changes within the microstructure.

Nanoindentation (NI) as a local probe technique allows testing small volumes as it is associated with tiny loads and small impression size. The high-resolution capability of such analytical tools makes it possible to study small scale mechanical properties of individual grains, across grain boundaries and of selected areas, like precipitates and strongly deformed grains. Reliable localized measurements are of great relevance for developing new alloys and nanocomposite materials. Besides the determination of mechanical parameters for practical engineering purposes, the origin and the mechanism of plastic deformation and cracking on the micro- and nanoscale in multiphase and small grain size materials might be studied. NI studies have already been performed on commercial Mg alloys, e.g. [4], and hardness changes by twinning were the central point of research in [5] on pure Mg.

Materials Processing

The Mg10GdxNd alloys investigated were prepared using a permanent mould direct chill casting technique at Helmholtz Zentrum Geesthacht, of which detailed information is given in [6]. The alloys containing Nd were solution treated (T4) at 525 °C for 24 h and quenched into water at room temperature. The ageing heat treatment (T6) was done on these alloys at 250°C for 6 h. The binary Mg10Gd alloy was directly extruded at the Extrusion Research and Development Center TU Berlin, at an overall temperature of 420 °C, an extrusion speed of 1 mm/s and a deformation degree φ of 1.6. Fig. 1a shows the as-cast microstructure revealing coarse dendritic grains up to 500 µm. Direct extrusion strongly decreases the grain size down to 15 µm due to recrystallization, see Fig. 1b. During heat treatment the dendritic microstructure disappears (Fig. 1c) and second phases are dissolved or activated to form fine precipitates, depending on T4 or T6.

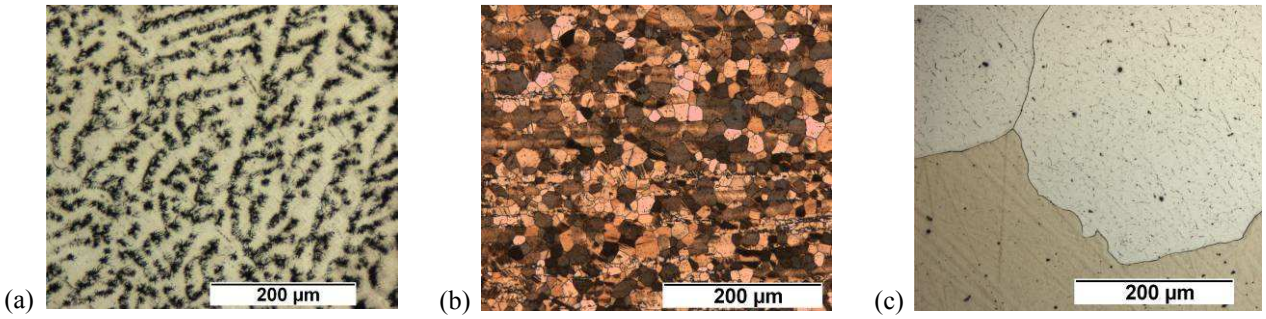

Fig. 1. Microstructure of Mg10GdxNd at different processing steps: (a) Mg10Gd as-cast, revealing dendritic casting microstructure, (b) Mg10Gd extruded, showing very fine grains after recrystallization and (c) Mg10Gd2Nd after solution heat treatment T4, where second phases are mostly dissolved and the dendritic microstructure has disappeared.

Experimental Procedures

NI measurements [7,8] were performed using the electrostatic transducer of the UBI 1Hysitron triboscope with a diamond 90° cube corner tip. Calibration of the tip was performed by the standard curve-fitting method using fused quartz with its known reduced modulus as the reference to determine the actual area function A_c as a function of the contact depth h_c [9]. Additionally, a commercial grid of ultra sharp conical silicon was used to get information about the indentation tip apex [10]. The blunt radius was determined as 250 nm. Indentation was achieved by single trapezoid load-time functions (holding segment of 10 s) and by multi-indentation with repeated loading and unloading at the same location on the sample surface [11]. This type of data collection method does not suffer from lateral inhomogeneities of the sample.

The measured data consisted of a load-displacement curve, which reflects the material response from the first indenter to sample contact down to the maximum penetration. The maximum load was varied between 500 µN and 3000 µN resulting in penetration depths of a few hundred nm. With the standard Oliver-Pharr method [9] the reduced or indentation modulus E_r and the hardness is calculated from the unloading part of the load-displacement curves. All measurements were carried out at room temperature in air. For Vickers hardness testing a fully automated Zwick/ZHU2.5/Z2.5 universal hardness testing machine with a HU measuring head, a microscope and motorized compound table was used for evaluation of HV0.2 and HV1 for comparison. Since there was no significant difference in HV values between these test loads of 1.961 N and 9.807 N, only HV0.2 values are presented within this paper.

Results and Discussion

Mechanical Properties. Table 1 presents the mechanical properties of the alloys which give the basic for additional hardness testing. These data were measured with a Zwick 050 testing machine with an initial strain rate of $1x10^{-3}$ mms^{-1}. It can be seen that increasing Nd increases the strength of

the as-cast condition F (solid solution) and applying solution treatment T4 decreases slightly the strength of Mg10Gd2Nd, whereas ageing (T6) strongly increases the strength. The strength of the extruded binary Mg10Gd alloy is higher compared to the as-cast alloy as a result of recrystallization.

Table 1. Tensile properties (TYS: tensile yield strength, UTS: ultimate tensile strength, El.: elongation to fracture) and Vickers hardness of Mg10Gd as-cast and extruded, Mg10Gd1Nd in F condition and Mg10Gd2Nd in F, T4, T6.

	Mg10Gd _F	Mg10Gd _extruded	Mg10Gd 1Nd_F	Mg10Gd 2Nd_F	Mg10Gd 2Nd_T4	Mg10Gd 2Nd_T6
TYS [MPa]	86.6	148.3	114.5	117.6	106.4	176.6
UTS [MPa]	131.2	251.2	162.4	160.2	162.1	224.6
El. [%]	2.5	19.42	2.5	1.2	2.9	0.8
Vickers hardness	69	92	72	72	66	95

Influence of Nd Content and Heat Treatment. Alloying Mg10Gd with Nd leads to improved strength and Vickers hardness in the as-cast condition compared to the binary alloy (Table 1). However, the properties are not significantly different when alloyed with 1 wt.% or 2 wt. % Nd. Fig. 2a shows also no significant difference between representative load-displacement curves (1 mN) of Mg10GdxNd in the as-cast condition. Nanohardness values (1.3 GPa and 1.34 GPa) and HV values (72 HV0.2) are similar increased from a nanohardness of 1.25 GPa and a Vickers hardness of 69 HV0.2 for the Mg10Gd as-cast alloy, see Table 2. NI offers the possibility to evaluate properties of very selective areas. A strong increase in nanohardness (average of 2.82 GPa) can be seen by testing second phase formations (Mg_5Gd precipitates) like that presented in Fig. 2b. Fig. 2a shows furthermore the influence of heat treatment; in this study applied to Mg10Gd2Nd. Solution treatment decreases nanohardness due to dissolving all second phases, whereas T6 aging increases nanohardness significantly. Apart form the load-displacement curves of Mg10Gd2Nd_T6 and the precipitate in Mg10Gd1Nd_F, all curves show pop-in effects at forces around 200 µN and 20 nm. These strain bursts are associated with the onset of plasticity; caused by nucleation and propagation of dislocations, see also [4].

Table 2 presents a good agreement of nanohardness with HV values, even to TYS in Table 1. However, if very selective areas, like precipitates, are of interest, HV testing has reached its limits; even at low loads (1.96 N) the indent size with 70 µm width is larger than the particle itself (5 µm).

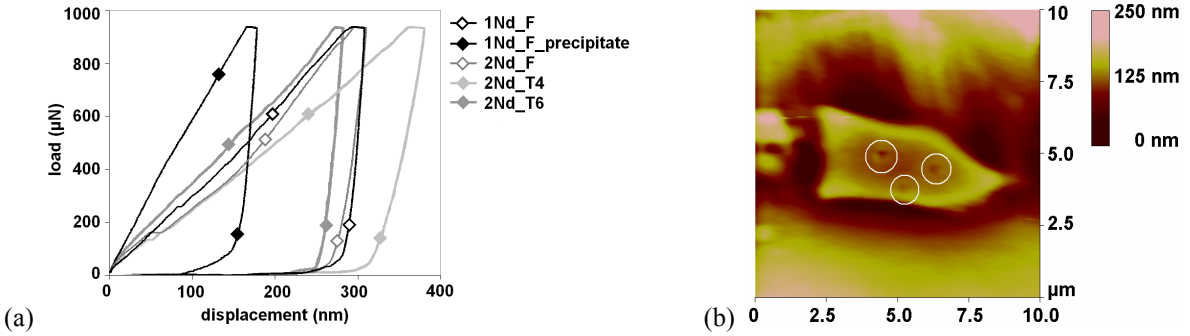

Fig. 2. (a) Load-displacement curves of Mg10GdxNd in different conditions: as-cast matrix, as-cast precipitate, T4 and T6, (b) Nanoindenter AFM image of an as-cast precipitate, nanohardness of 3 indents: 2.77 GPa, 2.80 GPa, 2.90 GPa.

Table. 2. Nanohardness (with a load of 1 mN) in comparison to HV0.2 of Mg10GdxNd: as-cast, T4 and T6.

	Mg10Gd _F	Mg10Gd 1Nd_F	Mg10Gd1Nd F_precipitate	Mg10Gd 2Nd_F	Mg10Gd 2Nd_T4	Mg10Gd 2Nd_T6
Nanohardness [GPa]	1.25	1.34	2.82	1.3	1.23	1.84
Vickers hardness	69	72	incapable to measure	72	66	95

Influence of Microstructure. Dendritic microstructures contain micropores and large grain sizes, which lead to a strong decrease in strength, hardness and creep resistance. Nanohardness values (correlated with Vickers hardness) shows lower values in hardness for as-cast material (Table 2). The nanohardness decreases towards the end of a dendritic arm and grain boundary, see Fig. 3a.

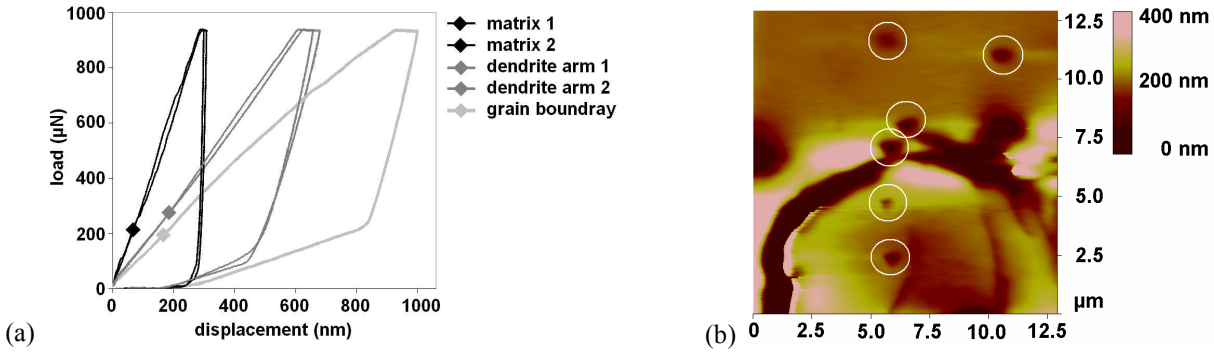

Fig. 3. (a) Load-displacement curves of Mg10Gd1Nd as-cast of the indents in (3b): matrix (H = 1.53 GPa), dendrite arm (H = 1.46 GPa), grain boundary (H = 1.27 GPa), (b) Nanoindenter AFM image of a grain boundary.

Grain refinement as a result of recrystallization leads to a strong increase in strength (Table 1) and also in Vickers hardness: Mg10Gd_F 69HV0.2 and Mg10Gd_extruded 92HV0.2, respectively. Table 3 reveals a nanohardness value of 1.8 GPa for the matrix material. The precipitates are found to be harder than the matrix, here only Mg_5Gd is forming. Due to the segregation of Gd into Mg_5Gd a depleted zone around the particle is expected. The low hardness value of 1.46 GPa agrees the conclusion that the matrix contains less Gd near the particle (less solid solution hardening).

Table. 3. Nanohardness (with a load of 500 µN) of extruded Mg10Gd dependening on indentation area: α-matrix, precipitate, depleted zone near a precipitate and in a twinned microstructure.

	Mg10Gd matrix	Mg10Gd grain boundary	Mg10Gd twin	Mg10G precipitate	Mg10Gd depleted zone
Nanohardness [GPa]	1.8	1.61	2.01	2.19	1.46

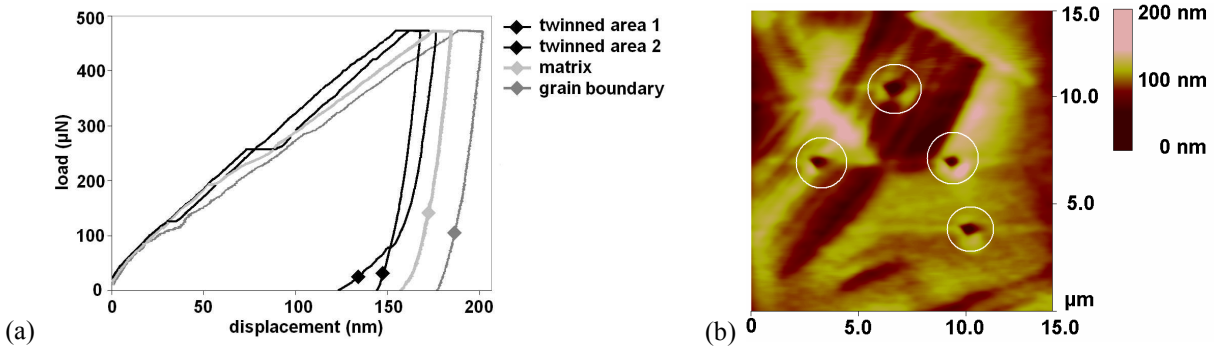

Fig. 4. (a) Load-displacement curves of Mg10Gd extruded of the indents in (4b): matrix - twins (pop-ins), precipitate, grain boundary, (b) Nanoindenter AFM image of the twinned area.

Mg alloys lead strongly to twinning during mechanical exposure. NI testing has been carried out on fracture samples after fatigue tests. Fig. 4a shows load displacement curves of twinned areas compared to non twinned material. Twinning, as a form of plastic deformation, increases the number of interfaces (twin boundaries) and causes strain hardening, which leads to a hardness increase; see the value of 2.01 GPa in Table 3. The Vickers indent size would be, as mentioned for the particles, much larger again, than the twinned grain itself. Grain boundaries as defected areas in the crystal show lower hardness, similar to that of the casting condition.

Although the extruded material is very fine grained, the scale of the indentation at the point where the first pop-in occurs is still smaller than the grain size. With testing grains and twins at these small scales the indenter very rarely encounters a grain boundary, and thus the pop-ins are

probably mostly associated with intragranular plasticity, which explains similar pop-in forces and depths. However, the overall hardness of the extruded material is higher compared to the casting condition due to increased dislocation density after work / strain hardening (extrusion, fatigue).

Summary

Nanoindentation has once more proven to be an excellent tool to test multiphase materials. Second phases could be tested in isolation and showed a very high nanohardness values. The increase in alloying element Gd within this particle left a depleted zone with lower hardness around it. Ageing heat treatment influences the nanohardness of cast Mg10GdxNd more strongly than increasing the Nd content from 1 to 2 wt. %. Precipitates, showing highest nanohardness values, are the most effective factor influencing the nanohardness, followed by twinning / grain size and solid solution.

As expected, there is an uncertainty in the indentation measurements, which can be caused by either the variation of the chemical composition in the different phases or by morphological effects, that are the grain and particle size as well as locally strain hardened areas. In particular, strain hardened areas after fatigue exposure have been found with higher hardness values due to an increase in interfaces because of twinning. The placement of the indent with respect to the particle boundary, the surface roughness, and the orientation effect are other crucial parameters. Besides these features in multiphase samples, there is a measuring uncertainty of the depth-sensing device itself, even when thermal drift, machine compliance, vibrations were attended with care.

Acknowledgements

The authors appreciate the support of Dr. Sören Müller (Extrusion Research and Development Center TU Berlin) for providing the extruded material and Dipl.-Ing. Ralf Tesch (UAS Stralsund) during Vickers hardness testing. Furthermore Dr. Chamini Mendis (HZG) is thanked for taking care of the heat treatment and Gerd Wiese (HZG) for supporting light optical metallographic preparation.

References

[1] L.L. Rohklin, Magnesium alloys containing rare earth metals, Taylor& Francis, London, 2003.

[2] B.L. Mordike, Mat. Sci. Eng. A 324 (2002) 103-112.

[3] N. Hort, Y. Huang, D. Fechner, M. Störmer, C. Blawert, F. Witte, C. Vogt, H. Drücker, R. Willumeit, K.U. Kainer, F. Feyerabend, Acta Biomater 6 (2010) 1714-1725.

[4] H. Somekawa, C.A. Schuh, Acta Mater. 59 (2011) 7554-7563.

[5] F. Hiura, R.K. Mishra, M. Lukitsch, M. Niewczas, Nano-indentation studies of twinned magnesium single crystals, in: S.N. Mathaudhu, W.H. Sillekens, N. R. Neelameggham, N. Hort (Eds.), Magnesium Technology 2012, The Minerals, Metals & Materials Society 2012, 117-119.

[6] F.R. Elsayed, N. Hort, M.A. Salgado-Ordorica, K.U. Kainer, Mater. Sci. Forum 690 (2011) 65-68.

[7] A.C. Fischer-Cripps, Nanoindentation, Springer-Verlag, New York, 2011.

[8] A. Richter, R. Smith, Encyclopedia Nanoscience and Nanotechnology 17 (2011) 375-438.

[9] W.C. Oliver, G. Pharr, J. Mater. Res. 7 (1992) 1562-1583.

[10] A. Richter, R. Smith, N. Dubrovinskaia, E. McGee, High Pressure Research 26 (2006) 99-109.

[11] B. Wolf, A. Richter, New J. Phys. 5 (2003) 15.1-15.17.